Chapter 6
Triplet-Emitter Doped Organic Materials

OLEDs have been extensively investigated for full-color, plat-panel display applications and illumination light sources because of their merits of high luminance, low driving voltage, and variety of emission colors [29]. The internal quantum efficiency of electro-fluorescence OLEDs is limited to around 25% according to simple spin statistics [36]. In order to overcome this efficiency limit of fluorescent OLEDs, phosphorescent emitters doped into host material have been used [312]. Phosphorescent emitters are low-molecular weight phosphorescent dye molecules incorporating a heavy metal atom with strong spin-orbit coupling that mixes singlet and triplet states. The radiative decay of triplet states becomes allowed and the efficiency of intersystem crossing is enhanced. As a result, the lowest triplet state is efficiently populated and produces light emission with a large quantum yield. Phosphorescent emitters in both small organic molecule hosts and polymer hosts allow for harvesting singlet and triplet excitons and, therefore, the internal quantum efficiency of OLEDs can be largely enhanced, approaching 100% [34].

In this chapter, triplet-emitter doped organic materials are studied. Section 6.1 focuses on the triplet dynamics and charge carrier trapping in triplet-emitter doped conjugated polymers. Phosphorescent properties and charge carrier trapping are studied by time-resolved photoluminescence and thermally-stimulated luminescence techniques. In Sect. 6.2, the use of triplet-emitters as lasing element is investigated. The results of Sect. 6.1 have been published in [311].

6.1 Triplet Dynamics and Charge Carrier Trapping in Triplet-Emitter Doped Conjugated Polymers

For the preparation of electro-phosphorescent polymer light-emitting diodes, the commonly used concept is to blend a low-molecular weight phosphorescent emitter into a proper polymer matrix. Transfer of excited state energy plays an important

S. Schols, *Device Architecture and Materials for Organic Light-Emitting Devices*,
DOI 10.1007/978-94-007-1608-7_6,

role in the operation of these devices. Singlet and triplet excitons can first be generated by electron-hole recombination in the polymer host and then transfer their energy to the dopant. Alternatively, the triplet state of the phosphorescent emitter may be formed by charge transfer from the host followed by charge recombination at the guest molecule. In both cases, the singlet and triplet energy levels of the host have to be well above the triplet state of the guest emitter to be efficient and prevent back transfer. The actual transfer of excitation to the guest molecule can occur via different mechanisms: Förster transfer of singlet excitons generated on the polymer matrix to the guest, Dexter transfer of both singlet and triplet excitons generated on the host to the dopant, as well as the direct generation of singlet and triplet excitons on the guest [313, 314].

Comprehensive studies have been performed to investigate triplet dynamics in MeLPPP doped by PtOEP[1] [307, 310, 315]. Since both the S_1 and T_1 levels of the dopant are below those of the matrix [316–318], both Förster-type host-guest singlet-singlet and Dexter-type triplet-triplet energy transfer can be envisaged. A specific feature of devices based on phosphorescence is that long phosphorescent lifetimes lead to saturation of emissive sites, and annihilation of triplet excitations may cause significant efficiency losses. Triplet-triplet annihilation is believed to be one of the major quenching mechanisms in phosphorescent OLEDs [266]. As a result, the efficiency of these OLEDs tends to decrease at high current densities [319]. The longer lifetime of triplet excitons also reduces one of the advantages of dye doping of organic light-emitting devices, namely the ability to eliminate concentration quenching. One way to solve these problems is to use dopants with shorter triplet exciton lifetime. Therefore Ir-complexes are more attractive candidates than platinum porphyrins owing to about one order of magnitude shorter lifetimes, which typically range from 1 to 14 μs [260].

In this section, we explore the phosphorescent properties of the red light-emitting metal-organic complex $Btp_2Ir(acac)$ doped into the conjugated polymer CNPPP. Similar to the above mentioned MeLPPP:PtOEP host-guest system, both the S_1 and T_1 levels of the $Btp_2Ir(acac)$ dopant are below those of the CNPPP polymer matrix; however, the phosphorescent lifetime of $Btp_2Ir(acac)$ ($\sim$7 μs [320]) is tenfold shorter than that of PtOEP ($\sim$80 μs [321]). It will be demonstrated that this results in different mechanisms dominating the phosphorescence properties. In addition, direct evidence that the phosphorescent metal-organic complexes do act as charge traps is presented and these traps are characterized by means of charge trapping spectroscopy. Polymer films doped with triplet-emitter molecules were prepared by dissolving the appropriate ratios of $Btp_2Ir(acac)$ and CNPPP in toluene, and then spin-coating the resulting solutions on a precleaned quartz substrate. The structural formulas of both compounds and the specific processing conditions used to prepare the organic thin films can be found in Chap. 2 (Sect. 2.1.1).

---

[1] Platinum(II) octaethyl porphyrin.

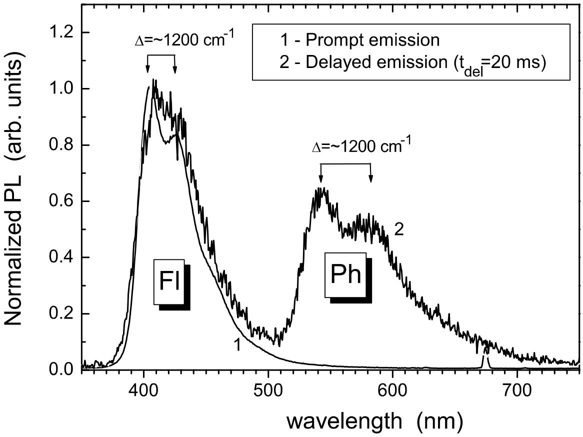

Fig. 6.1 Normalized spectra of prompt fluorescence (curve 1) and delayed emission (curve 2) from a pristine CNPPP film at 80 K. Delayed emission was measured with 20 ms delay time after the laser pulse and with a gate width of 6 ms. (© Elsevier)

6.1.1 Spectroscopic Characterization

Pristine CNPPP Films

Figure 6.1 (curve 1) shows the prompt fluorescence spectrum of a pristine CNPPP film registered during the laser pulse at 80 K. The spectrum consists of a main $S_1 \rightarrow S_0$ band at 405 nm (3.08 eV) followed by a vibronic feature displaced by about 1200 cm^{-1}. This spectrum coincides with steady-state PL spectra, implying that the fluorescence in the range of 400–500 nm, caused by the radiative decay of singlet excitons, is dominant in this material.

The delayed emission spectrum of the pristine CNPPP film, detected by introducing a time delay ($t_{del} = 20$ ms) between the exciting laser pulse and the detection window of the registration system, is depicted by curve 2 in Fig. 6.1. In contrast to prompt fluorescence, the delayed emission from CNPPP exhibits two different components with different decay times and different spectral positions. The short wavelength component of the delayed emission is virtually identical to the prompt fluorescence spectrum. Consequently, it can be assigned to delayed fluorescence (DF) from the S_1 state of CNPPP. The second, slower decaying set of bands is shifted by 0.78 eV with respect to the first peak of the DF, but has the same vibronic splitting of about 1200 cm^{-1} (Fig. 6.1, curve 2) as the fluorescence spectrum. It should be noted that this second longer-wavelengths spectral component can only be seen in the delayed emission and shows all generic signatures of phosphorescence, principally similar to that previously found in other conjugated polymers as MeLPPP [322, 323], LPPPC[2] [324] and polyfluorenes [308]. Therefore, this spectral part in the range of 520–700 nm (Fig. 6.1, curve 2) is assigned to intrinsic phosphorescence (Ph) from the T_1 state at 542 nm (2.3 eV). Pristine CNPPP thus features a singlet-triplet (S_1-T_1) energy level splitting of about $\Delta E_{ST} = 0.78$ eV, which is a typical value for organic conjugated polymers [306].

---

[2] Ladder-type poly(para-phenylene carbazole).

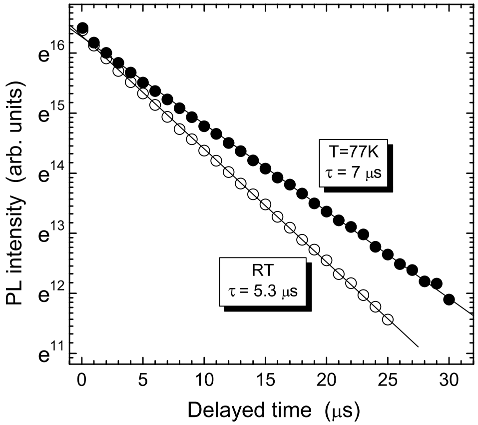

Fig. 6.2 Time decay kinetics of Ph emission measured in a PS:(1 wt%)$Btp_2Ir(acac)$ film at 77 K and room temperature. The gate width was 0.1 μs. (© Elsevier)

$Btp_2Ir(acac)$ Doped into a PS Matrix

In order to get an insight into the intrinsic Ph properties of $Btp_2Ir(acac)$, the CW- and time-resolved PL of this triplet-emitter doped into a polystyrene (PS) film has been studied. Because PS did not show any light emission under the excitations used in this study, it can be considered as an optically inert polymer host allowing matrix isolation of $Btp_2Ir(acac)$ molecules. Therefore, Ph properties of PS:$Btp_2Ir(acac)$ films are virtually the same as those measured in frozen diluted solution. The Ph decay kinetics of a $Btp_2Ir(acac)$ (1 wt%) doped PS film recorded at 77 K and room temperature are depicted in Fig. 6.2. The Ph decay curves demonstrate a clear mono-exponential kinetics, indicating that the triplet excitations of $Btp_2Ir(acac)$ are efficiently confined by the PS host at such dopant concentration and that triplet quenching by impurities or via T-T-annihilation mechanism is negligible. The intrinsic lifetime of Ph emission decreases from 7 μs at 77 K to about 5 μs when the temperature increases to room temperature. This correlates with the observed gradual decrease of the Ph intensity of $Btp_2Ir(acac)$ with elevating temperature (Fig. 6.3) and suggests that temperature-dependent non-radiative processes are active in this metal-organic complex [320].

Figure 6.4 presents the low-temperature Ph decay kinetics of $Btp_2Ir(acac)$ doped PS films at small and relatively high dopant concentration (1 and 10 wt%). As can be seen, the apparent Ph lifetime is notably smaller ($\tau = 5.3$ μs) at 10 wt% $Btp_2Ir(acac)$ concentration compared to a concentration of 1 wt% ($\tau = 7$ μs). This quenching is definitely related to the dopant concentration (concentration quenching) and not to T-T annihilation as verified by the linear intensity dependence of Ph in PS:(10 wt%)$Btp_2Ir(acac)$ upon excitation intensity (inset of Fig. 6.4).

Figure 6.5 shows the profile of the first Ph band ($T_1 \rightarrow S_0$) from $Btp_2Ir(acac)$ in a frozen diluted toluene solution ($c = 10^{-3}$ wt%) and from $Btp_2Ir(acac)$ doped in a PS film at $c = 10$ wt% measured at different delay time (Fig. 6.5(a) and (b), respectively). The Ph peak position of $Btp_2Ir(acac)$ in frozen solution showed no peak shift (Fig. 6.5(a)), whereas in heavily doped PS films, a gradual red-shift of the peak with increasing delay time (Fig. 6.5(b)) was observed. The same red-shift was

Fig. 6.3 Ph intensity of a 1 wt% $Btp_2Ir(acac)$ doped PS film measured at different temperatures. At elevated temperatures a decrease of the Ph yield is observed. (© Elsevier)

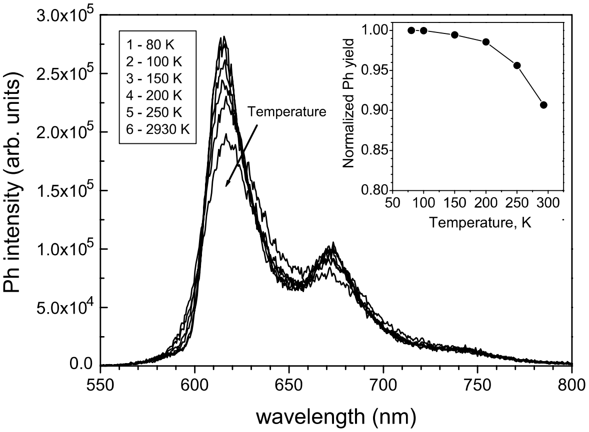

Fig. 6.4 Time decay kinetics of Ph emission measured in PS:$Btp_2Ir(acac)$ films at 1 and 10 wt% concentrations of $Btp_2Ir(acac)$. The kinetics were measured at 80 K with a gate width of 0.1 μs. *Inset*: dependence of the Ph intensity in a PS:(10 wt%) $Btp_2Ir(acac)$ film upon the laser excitation intensity. (© Elsevier)

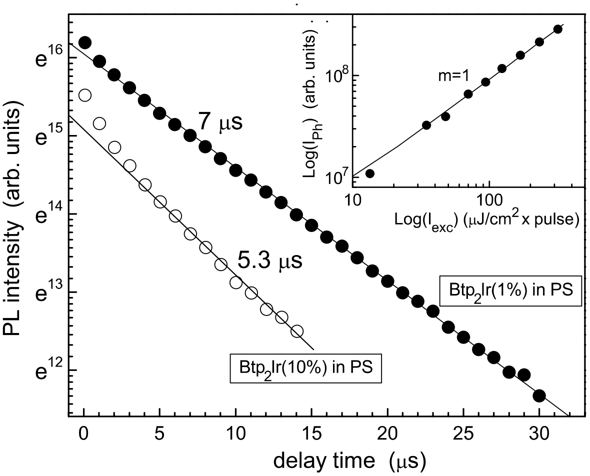

observed for the vibronic replica peaks (not shown here). This shift is a direct observation of the so-called spectral diffusion effect of the Ph spectra of $Btp_2Ir(acac)$ and is the result of triplet migration from one excited state to another during the triplet lifetime. Since triplet diffusion towards excited states with a lower energy is favored (downward hopping), a red-shift of the Ph peak is observed. This process is schematically illustrated in Fig. 6.6.

The observation of spectral diffusion proves that triplets can migrate through the $Btp_2Ir(acac)$ molecules manifold at a doping level of 10 wt%. It actually implies that triplets are no longer confined on isolated $Btp_2Ir(acac)$ molecules at such doping concentration, which is close to that often used for fabrication of high-efficiency phosphorescent OLEDs [321]. Consequently, at such a concentration, the triplets could be amenable to quenching. Indeed, minor traces of quenching impurities, such as triplet molecular oxygen or some intrinsic quenching defects in the PS polymer,

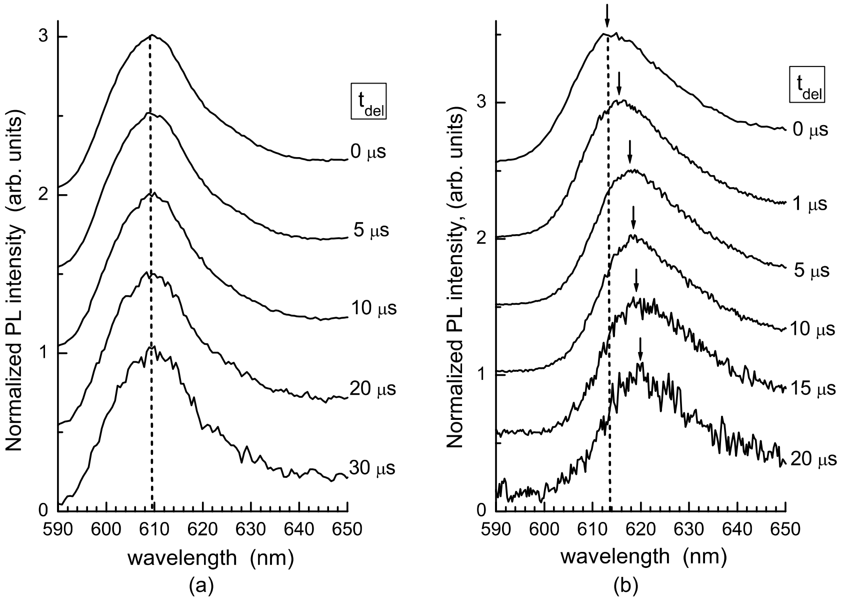

Fig. 6.5 (**a**) Time resolved first Ph peak from $Btp_2Ir(acac)$ in a frozen diluted toluene solution ($c = 10^{-3}$ wt%), and (**b**) Time resolved first Ph peak from $Btp_2Ir(acac)$ doped in a PS film at $c = 10$ wt%. All spectra were measured at 80 K and normalized to the peak intensity. (© Elsevier)

Fig. 6.6 Schematical illustration of the spectral diffusion effect. (© Elsevier)

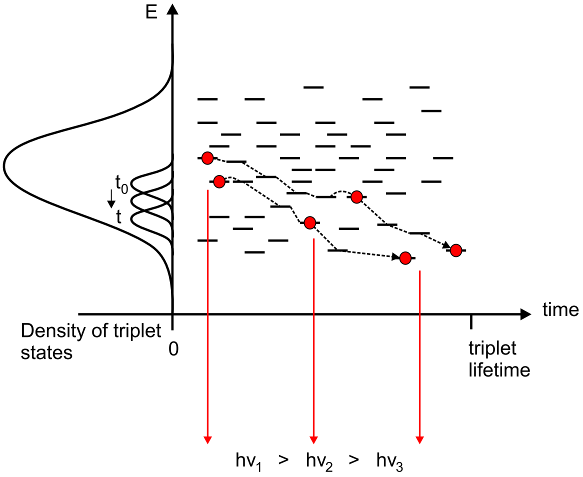

could become accessible to migrating triplets within the radiative lifetime of the triplet excitation [323].

In general, short-range Dexter energy transfer dominates migration of triplet excitations. The observation of triplet migration at a $Btp_2Ir(acac)$ concentration of 10 wt% is, however, in good agreement with the recently proposed mechanism of dipole-dipole long-range Förster energy transfer in phosphorescent Ir(III) complexes [325]. Kawamura *et al.* found out that the strong spin-orbital coupling in these compounds increases the oscillator strength of the triplet-singlet transition and leads to a sufficiently high dipole-dipole transfer rate to enable Förster energy transfer to be the dominant mechanism in these phosphorescent Ir-complexes [325]. An effective Förster radius of 1.5 nm was calculated for $Btp_2Ir(acac)$ [325]. The average distance between the $Btp_2Ir(acac)$ molecules in a PS host at a doping concentration of 10 wt% is $\rho = 2.2$ nm. This value was calculated using the so-called lattice gas model [326]:

$$\rho = \left(\frac{M}{N_A c \delta} \right)^{1/3}, \tag{6.1}$$

where M is the $Btp_2Ir(acac)$ molecular weight, N_A is the Avogadro's constant, c is the fractional $Btp_2Ir(acac)$ concentration and δ is the sample density. Taking into account that Eq. 6.1 gives the average distance between the center of the molecules and thus slightly overestimates the intermolecular distance, 2.2 nm, determined above, is not very different from the effective Förster radius obtained by Kawamura. Förster energy transfer might thus indeed explain the spectral diffusion effect observed in the present study at 10 wt% dopant concentration (Fig. 6.5(b)).

The results presented in Fig. 6.5 elucidate the observed apparent decrease of the exciton lifetime of $Btp_2Ir(acac)$ at increased dopant concentration in PS films (Fig. 6.4). If triplet excitons are no longer confined on individual $Btp_2Ir(acac)$ molecules at 10 wt% dopant concentration, as proven by the observed spectral diffusion effect, the probability of triplet quenching by accidental impurities, which is suppressed in a highly diluted system, increases with concentration, giving rise to the observed concentration quenching effect. The quenching impurity is most probably triplet molecular oxygen, which is a notoriously efficient triplet exciton quencher. Comparison of the Ph decay kinetics in oxygen-free encapsulated films and that of films exposed to the ambient atmosphere strongly supports such a notion. Figure 6.7 shows the low-temperature Ph decay kinetics of PS:$Btp_2Ir(acac)$ films at high (10 wt%) triplet-emitter concentration. As can be seen, oxygen-free (never exposed to air and encapsulated in the glove-box) films (Fig. 6.7, curve 1) show the same mono-exponential Ph decay with a lifetime of 7 μs as for diluted systems, suggesting negligible triplet quenching in them. On the other hand, PS:(10 wt%)$Btp_2Ir(acac)$ films exposed to air feature an initial fast non-exponential decay (curve 2), which is a clear indication of quenching by oxygen. In combination with the results presented in Fig. 6.5, this suggest straightforwardly that the concentration quenching in PS:$Btp_2Ir(acac)$ systems arises due to triplet exciton migration at increased guest molecule concentration and thus due to their ability to encounter non-radiative oxygen impurities.

It should be mentioned that a significant phosphorescence lifetime shortening due to oxygen was recently reported [307] for another host-guest system, namely MeLPPP doped with PtOEP (concentration from 10^{-3} to 5 wt%). The effect was explained by reversible formation of a weak complex between PtOEP and oxygen upon exposing the sample to air, which quenches the phosphorescence of PtOEP. It

Fig. 6.7 Low-temperature Ph decay kinetics of a PS:(10 wt%)$\mathrm{Btp_2Ir(acac)}$ film encapsulated between two quartz plates in the glovebox (curve 1) and for a film prepared from the same solution but exposed to the air before loading to the cryostat (curve 2). (© Elsevier)

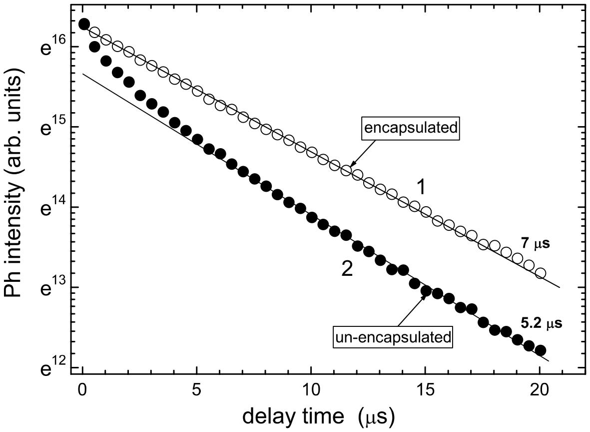

was assumed that not mobile but localized guest triplets are involved in the quenching effect [307]. In our study, however, it is observed that the oxygen quenching effect on the phosphorescence of $\mathrm{Btp_2Ir(acac)}$ depends strongly on the guest concentration (Fig. 6.4), as no notable lifetime shortening was found at 1 wt% $\mathrm{Btp_2Ir(acac)}$ concentration either in a PS (Fig. 6.4) or CNPPP (see further down, Fig. 6.9(b)) host matrix, while at a larger (10 wt%) dopant concentration the quenching effect was obvious. The remarkable correlation of the quenching effect with the onset of the spectral diffusion of the phosphorescence of $\mathrm{Btp_2Ir(acac)}$ dispersed in a polymer matrix proves that in the present experiment, using $\mathrm{Btp_2Ir(acac)}$ dopants, mobile triplets are involved and that they are able to reach the oxygen quenching center at sufficiently large dopant concentration. This discrepancy might be rationalized by taking into account the considerably shorter intrinsic phosphorescence lifetime of $\mathrm{Btp_2Ir(acac)}$ (7 μs vs. ~80 μs for PtOEP) and, consequently, the somewhat larger oscillator strength of the radiative transition in this organometallic complex as compared to PtOEP molecule.

Finally, it should be noted that the presented results suggest that the concentration quenching effect, at least at 10 wt% $\mathrm{Btp_2Ir(acac)}$ concentration level, is definitely due to quenching by impurities like molecular oxygen and not due to the mechanism based on dampening of energy through multiple dipole-dipole energy exchange interaction between neighboring Ir-complex molecules as was suggested before [325]. Indeed, Fig. 6.5(b) proves that triplet energy migration does occur at this dopant concentration, but oxygen-free encapsulated PS:(10 wt%)$\mathrm{Btp_2Ir(acac)}$ films do not show any shortening of the triplet lifetime (Fig. 6.7). An energy dampening mechanism [325, 327] may, however, still be operative at smaller average distances between $\mathrm{Btp_2Ir(acac)}$ molecules (i.e. at larger dopant concentrations).

CNPPP Films Doped with $\mathrm{Btp_2Ir(acac)}$

Figure 6.8(a) shows the normalized steady-state low-temperature PL spectra of CNPPP films doped with $\mathrm{Btp_2Ir(acac)}$ at different doping concentrations. As can

Fig. 6.8 (**a**) Steady-state PL spectra of CNPPP films doped with $\text{Btp}_2\text{Ir(acac)}$ at doping concentration of 1 and 6 wt% measured at 80 K, and (**b**) EL spectra of CNPPP:$\text{Btp}_2\text{Ir(acac)}$ films with doping concentration varying from 1 to 6%. (© Elsevier)

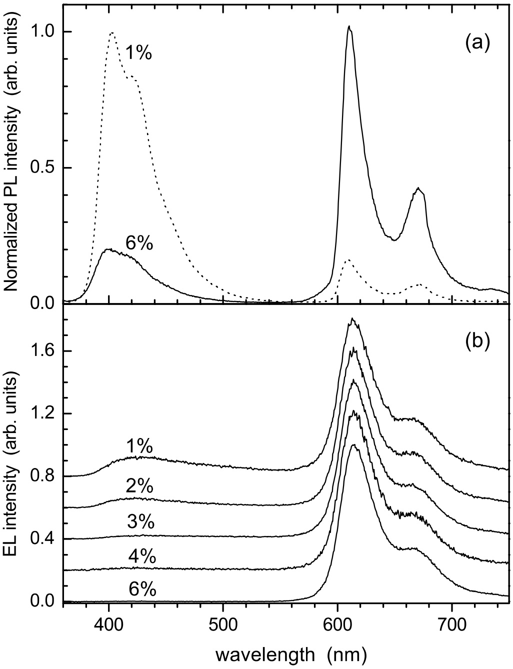

be seen, the PL spectra exhibit two components corresponding, respectively, to fluorescent emission from the CNPPP host in the range from 400 to 500 nm, and a set of red emission peaks of $\text{Btp}_2\text{Ir(acac)}$ phosphorescence. The phosphorescence (Ph) of $\text{Btp}_2\text{Ir(acac)}$ shows a well-resolved spectrum with the $T_1 \rightarrow S_0$ band at 610 nm (2.05 eV), followed by a vibronic fine structure. The mechanism of Ph in this compound has been assigned before to the transition from ligand-based triplet $^3(\pi - \pi^*)$ states [260, 321]. Time-resolved PL studies of pure CNPPP films (Fig. 6.1, curve 2) have revealed the intrinsic phosphorescence in this polymer and allow direct estimation of the triplet energy of 2.3 eV in this material. Since this CNPPP triplet level exceeds the guest triplet level at 2.05 eV, efficient confinement of $\text{Btp}_2\text{Ir(acac)}$ triplet excitations is possible in the CNPPP:$\text{Btp}_2\text{Ir(acac)}$ host-guest system. Clearly, the relative contribution from the fluorescence emission of the CNPPP host reduces significantly with increasing $\text{Btp}_2\text{Ir(acac)}$ concentration. This is expected due to Förster singlet energy transfer from the host matrix to the dopant, followed by intersystem crossing to the triplet state of the iridium complex [328]. However, even at dopant concentrations as high as 6 wt% the host fluorescence is not completely quenched (Fig. 6.8(a)). Note that light absorption at the excitation wavelength $\lambda_{exc} = 337$ nm in CNPPP:$\text{Btp}_2\text{Ir(acac)}$ thin films is dominated by CNPPP host absorption at all considered dopant concentrations. Therefore, excitation of $\text{Btp}_2\text{Ir(acac)}$ molecules could only be possible via energy transfer from the host matrix.

The electroluminescence (EL) spectra of $\text{Btp}_2\text{Ir(acac)}$ doped CNPPP films are shown in Fig. 6.8(b). These spectra were measured at different $\text{Btp}_2\text{Ir(acac)}$ doping concentration and by using an ITO/PEDOT/CNPPP:$Btp_2Ir(acac)$/LiF/Al device configuration. As can be seen, in contrast to the PL emission spectra (Fig. 6.8(a)), a complete quenching of the host EL emission occurs at notably lower $Btp_2Ir(acac)$ doping concentration (as low as 3 wt%). EL quenching commonly occurs at much lower triplet emitter concentration as compared to the PL emission and has been attributed by many authors to charge recombination taking place preferentially on triplet emitter molecules, tacitly assuming efficient charge-carrier trapping by the dopant species [328, 329].

The intensity dependence of prompt fluorescent and Ph emission of CNPPP films doped with 1 wt% $Btp_2Ir(acac)$ upon laser excitation intensity is presented in Fig. 6.9(a). The plotted emission intensities were obtained by integration over the wavelength. The CNPPP fluorescence intensity varies approximately linearly with the laser power (curve 1). The Ph of $Btp_2Ir(acac)$, on the other hand, behaves in a different way (Fig. 6.9(a), curve 2): at low excitation intensity the dependence of Ph is a linear function ($I_{ph} \sim I_{exc}^m$, where $m = 1$), whereas at power excitation densities higher than ∼50 μJ/(cm^2 pulse) a crossover to a slow square-root increase ($m = 0.5$) occurs. Such intensity dependence of Ph at high excitation densities usually arises from a bimolecular quenching process which competes with the monomolecular decay and is often considered as a signature of triplet-triplet annihilation (T-T-annihilation) ($T_1 + T_1 \rightarrow S^* + S_0$) [308, 323], implying a decrease of the Ph yield at high pump fluence. The slow square-root increase with increasing excitation intensity cannot be related to the host singlet state since the fluorescence of this host-guest system does not show saturation behavior (Fig. 6.9(a), curve 1). In addition, it was found that the excitation intensity at which the above crossover is observed shifts to somewhat lower intensities with increasing temperature, as expected for a thermally activated diffusion migration of triplet excitations governing the T-T annihilation.

Figure 6.9(b) shows the decay kinetics of phosphorescent emission of $Btp_2Ir(acac)$ in the same CNPPP:(1 wt%)$Btp_2Ir(acac)$ film as in Fig. 6.9(a) measured at low- and high- laser excitation intensity at 80 K (curve "a" and "b", respectively). The excitation intensities used are indicated by arrows in Fig. 6.9(a) and these laser powers correspond to the regime of either a linear- or a square-root-Ph increase with increasing pump intensity. At low excitation intensity the Ph of $Btp_2Ir(acac)$ doped in a CNPPP matrix decays mono-exponentially over the studied time range, featuring a lifetime of about $\tau = 7$ μs (Fig. 6.9(b), curve "a"). This observation, which is virtually the same as has been observed in an optically inert PS host (Fig. 6.9(b), open symbols) at 1 wt% dopant concentration, indicates that the CNPPP host indeed can efficiently confine triplet excitations of $Btp_2Ir(acac)$ molecules. At high excitation intensity (Fig. 6.9(b), curve "b"), on the other hand, the decay kinetics deviate from a single exponent; a fast initial Ph decay during several microseconds after the laser pulse is followed by a mono-exponential decay with the same lifetime of 7 μs at larger delay times. This behavior proves that efficient bimolecular T-T annihilation occurs during the first 10 μs after the laser pulse when the concentration of triplets in the material is still large enough. T-T annihilation leads to the depletion of the reservoir of triplet excitations and therefore the de-

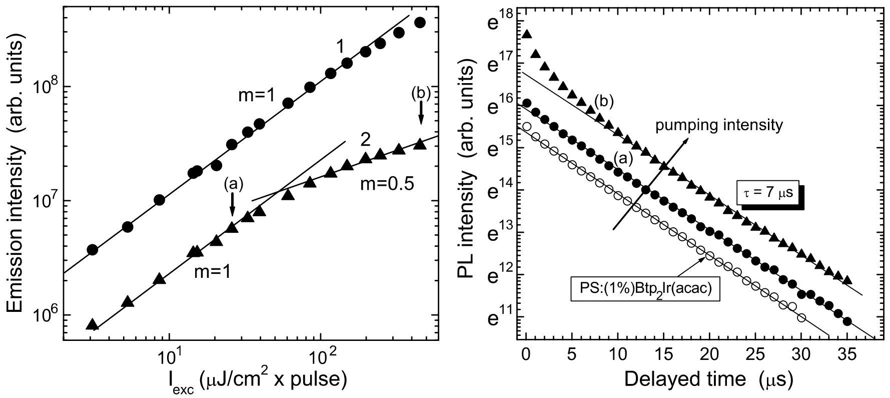

(a) (b)

Fig. 6.9 (**a**) Dependence of CNPPP host fluorescence (curve 1) and Btp$_2$Ir(acac) guest phosphorescence (curve 2) upon excitation intensity at 80 K in a CNPPP:(1 wt%)Btp$_2$Ir(acac) film. The *arrows* depict the low- and high- laser power intensities at which the Ph decay kinetics presented in Fig. 6.9(b) have been measured. (**b**) Time decay kinetics of Ph emission measured in a CNPPP:(1 wt%)Btp$_2$Ir(acac) film at low- and high- laser excitation intensity at 80 K (curve (a) and (b), respectively). The gate width was 0.1 μs. The Ph decay kinetics at 80 K of 1 wt% Btp$_2$Ir(acac) doped into a polystyrene film are given by *open circles* (this curve is arbitrary shifted on the ordinate scale). (© Elsevier)

cay kinetics in this time domain do not follow an exponential decay law. Upon lowering the triplet concentration at $t_{del} > 10$ μs the kinetics become mono-exponential again. The onset of the T-T annihilation process has been straightforwardly observed in the Ph intensity dependence measurements of Fig. 6.9(a). It should be noted that no deviation from the mono-exponential Ph decay with $\tau = 7$ μs was observed when Btp$_2$Ir(acac) was doped into a PS film, irrespective of the laser excitation intensity level (Fig. 6.9(b), open cycles).

The excitation intensity effect on the Ph yield was studied recently for PtOEP doped in MeLPPP and the Ph yield was found to decrease at high intensity of the incident light [307]. The observed saturation effect of the dopant phosphorescence at intensities exceeding ~10 μJ/(cm^2 pulse) was virtually the same regardless whether PtOEP was doped into MeLPPP or into an optically neutral PS matrix and the phenomenon was explained in terms of bleaching of ground-state PtOEP molecules upon population of their triplet state [307]. Such an explanation is definitely not applicable to the Ph intensity dependence of CNPPP:Btp$_2$Ir(acac) observed in the present study as the dominance of bleaching is at variance with (i) the observation of the obvious deviation of the Ph decay kinetics from a single exponent at high excitation intensities (Fig. 6.9(b)), which, on the other hand, nicely agrees with the T-T annihilation mechanism; (ii) no decrease of Ph yield of Btp$_2$Ir(acac) was found when it was embedded in a neutral PS matrix and in frozen diluted solution up to the pumping intensity of ~500 μJ/(cm^2 pulse); (iii) the crossover from a linear to square-root increase of the Ph intensity dependence in the CNPPP:Btp$_2$Ir(acac) host-guest system tends to shift to lower pumping intensities with increasing temperature, thus pointing to the importance of triplet exciton diffusion. Hence, the reduction of the Ph yield in the CNPPP:Btp_2Ir(acac) system at high excitation intensity is most probably governed by T-T annihilation, which predominates over the possible bleaching effect of the Btp_2Ir(acac) ground-state. The latter effect in the present system might certainly be possible at larger excitation intensity.

The question arises which triplets, of the host or of the guest, are responsible for the T-T annihilation quenching in the CNPPP:Btp_2Ir(acac) system. The results obtained on Btp_2Ir(acac) doped into a PS or a CNPPP host matrix suggest that at 1 wt% doping the guest triplet excitations must be confined by both polymer hosts. At such low concentration, guest triplet migration is not possible, in other words, guest triplets are immobile. Therefore, T_{guest}-T_{guest} annihilation is impossible. On the other hand, all CNPPP host triplet excitons are eventually transferred to the phosphorescent guest as proven by the complete quenching of the intrinsic CNPPP phosphorescence (see further down, Fig. 6.10). This precludes T_{host}-T_{host} annihilation at not very small dopant concentration. Therefore, we conclude that the observed T-T annihilation proceeds via a T_{guest}-T_{host} annihilation reaction, i.e., when a mobile host triplet encounters a localized guest triplet excitation. This picture is in agreement with the absence of T-T annihilation quenching for Btp_2Ir(acac) doped in a PS host matrix at the same concentration level, since excited host triplets are missing in this case. It should be mentioned that bimolecular hetero-annihilation between triplet excitons of a polymer and triplet excitations of dopants has already been reported before for MeLPPP:PtOEP host-guest systems [310].

Figure 6.10 presents time-resolved PL spectra of a CNPPP film doped with 0.05 wt% Btp_2Ir(acac) recorded at 80 K over a very wide range of delay times after the laser pulse excitation (from 0.1 μs to 800 μs) and employing a large width of 1 ms of the gate window (so-called integration mode). As can be seen, both the DF of the host and the Ph of the dopant contribute to the delayed emission spectra. However, no intrinsic Ph of the CNPPP host at 542 nm (Fig. 6.1) could be observed in the CNPPP:Btp_2Ir(acac) host-guest system, implying that the host triplet excitations are efficiently quenched by the lower-energy Btp_2Ir(acac) triplet state via Dexter mechanism. With increasing Btp_2Ir(acac) concentration a reduction of the delayed fluorescence intensity of the polymer host has been observed.

The time dependence of the DF and Ph intensity in the CNPPP:Btp_2Ir(acac) host-guest system is shown in the inset of Fig. 6.10. A remarkable observation is that the Ph of Btp_2Ir(acac) in a CNPPP matrix can be measured even at delay times that are orders of magnitude larger than the intrinsic Ph lifetime of Btp_2Ir(acac) ($\sim$7 μs). As can be seen, after the initial decay of the relatively short-lived guest phosphorescence featuring a lifetime of 7 μs at 80 K, the Ph decay kinetics show a very long tail lasting up to milliseconds. This observation of "delayed phosphorescence" may have two plausible origins: (i) delayed arrival of intrinsically long-lived host triplets to the Btp_2Ir(acac) guest molecules, or (ii) delayed production of guest triplets by delayed recombination of (trapped) charge carriers on Btp_2Ir(acac) guest molecules.

Besides delayed guest Ph, intensive delayed fluorescence (DF) of the CNPPP host has also been observed in the delayed emission spectra of CNPPP:(0.05 wt%)Btp_2Ir(acac) films (Fig. 6.10). The DF in these films (as well as in pristine

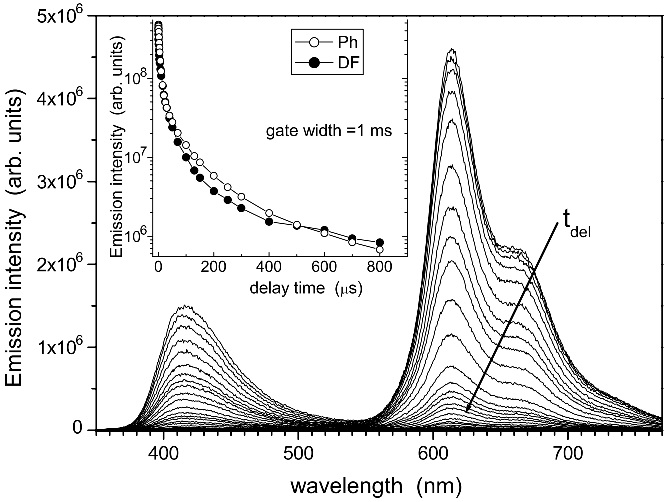

Fig. 6.10 Time-resolved PL spectra of a CNPPP film doped with 0.05 wt% $Btp_2Ir(acac)$ at 80 K. The delay time t_{del} varies from 0.1 μs to 800 μs at a constant gate width of 1 ms. The *inset* shows the time dependence of the DF and Ph intensity in the CNPPP:$Btp_2Ir(acac)$ host-guest system. (© Elsevier)

CNPPP films) arises most probably due to T_{host}-T_{host} annihilation as (i) the intensity dependence of the DF varies almost quadratically with the excitation laser intensity (not shown here), implying a bimolecular mechanism of population of the singlet level, (ii) Ph of the guest is a linear function of the pumping intensity, and (iii) the CNPPP film shows intrinsic long-lived triplet excitations detected even in the millisecond time domain (Fig. 6.1). These factors seem to favor the mechanism of delayed arrival of host triplets as the main cause for delayed phosphorescence. However, at higher $Btp_2Ir(acac)$ concentration the DF emission of the host decreases dramatically. This is in good agreement with the mechanism of T_{host}-T_{host} annihilation as source of the DF. Indeed, as guest molecules readily accept triplets from the host, it is expected that the apparent host triplet lifetime and their population strongly decreases with increasing guest concentration. Consequently, the intensity of delayed T_{host}-T_{host} annihilation, and therefore DF, is reduced at higher doping concentrations. On the other hand, increasing the $Btp_2Ir(acac)$ dopant concentration has almost no effect on the delayed phosphorescence in CNPPP:$Btp_2Ir(acac)$ films. The decay kinetics of the long-lived component (delayed phosphorescence) were found to be virtually the same for different $Btp_2Ir(acac)$ dopant concentrations ranging from 0.05 to 5 wt%. For the mechanism based on delayed arrival of host triplet excitations one should contrarily expect that the decay of the above slow component (delayed phosphorescence) becomes much faster with increasing dopant concentration because quenching of host triplets by triplet-emitter dopants is considerably enhanced in such case. Therefore, we are forced to conclude that the delayed production of guest triplets occurs mainly via delayed recombination of charge carriers on $Btp_2Ir(acac)$. Such an efficient delayed charge-carrier recombination could be ensured by trapped charge carriers and is most probably the dominant mechanism for the delayed $Btp_2Ir(acac)$ phosphorescence. To elucidate the origin of charge trapping in the CNPPP:$Btp_2Ir(acac)$ host-guest system thermally stimulated luminescence (TSL) experiments have been performed.

6.1.2 Thermally Stimulated Luminescence in CNPPP Doped with $Btp_2Ir(acac)$

Figure 6.11 presents the TSL glow curve of a CNPPP film doped with $Btp_2Ir(acac)$ (solid curve). As can be seen, TSL of CNPPP:$Btp_2Ir(acac)$ contains two major peaks, namely a low-temperature peak near 50 K and a high-temperature one with a maximum at 220 K. TSL of a pristine CNPPP film is shown for comparison (dashed curve) and is dominated by the low-temperature TSL peak at 50 K while another weaker peak emerges at $\sim$150 K. It should be mentioned that a similar low-temperature peak centered at 45–50 K has been commonly observed in many conjugated polymers such as MeLPPP [242], polyfluorenes [309], PPV derivatives [243], etc. and it arises due to charge carrier release from the tail states of the intrinsic density-of-state (DOS) distribution of the polymer. The weaker TSL feature at 150 K in pristine CNPPP film (dashed curve) is quite similar to the one observed in polyfluorene polymers [309] and its relative intensity is rather sensitive to film preparation conditions. This weak peak is due to moderately deep inherent charge traps in the CNPPP film, which could be of structural origin in this material. It might be related to some sort of aggregates of polymer chains as it was found before for substituted polyfluorenes [309] and PPV derivatives [243]. As evidenced from Fig. 6.11, doping of the CNPPP host with $Btp_2Ir(acac)$ results in the appearance of a new high-temperature TSL peak at 220 K, suggesting that $Btp_2Ir(acac)$ molecules create rather deep traps in the polymer matrix. The activation energy of this deep trap is about 0.6 eV, as measured by the fractional TSL technique, and agrees well with the difference between the HOMO level of CNPPP and that of $Btp_2Ir(acac)$ which are, respectively, 5.7 [239] and 5.0 eV [240]. Hence, TSL trapping spectroscopy provides a direct evidence that $Btp_2Ir(acac)$ phosphorescent complexes create relatively deep hole traps in the CNPPP matrix. Electron trapping by $Btp_2Ir(acac)$ is not possible because the LUMO of the dopant (2.2 eV [240]) is higher than the one of the polymer matrix (2.3 eV [239]).

The fact that $Btp_2Ir(acac)$ complexes act as hole traps in CNPPP, support our argumentation that the delayed production of guest triplets occurs mainly via delayed recombination of charge carriers and may explain the observation of delayed phosphorescence (Fig. 6.10). When a hole is trapped on $Btp_2Ir(acac)$ molecules and an electron is localized on some shallower intrinsic traps of the CNPPP polymer, trapped geminate electron-hole pairs can be readily generated. Such trapped geminate pairs are typically more stable against recombination compared to non-trapped electron-hole pairs and depending on mutual separation between opposite sign charge carriers they can survive for milliseconds or even seconds [242, 330].

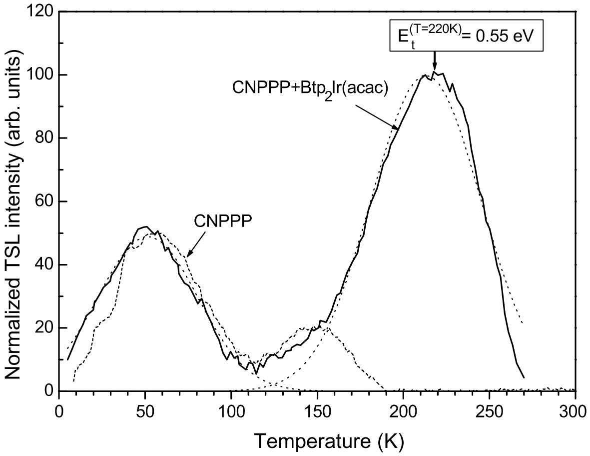

Fig. 6.11 The TSL glow curve of a CNPPP film doped with 5 wt% Btp$_2$Ir(acac) (*full line*) and pristine CNPPP film (*dashed line*) after excitation with 365 nm light at 4.2 K. (© Elsevier)

Since recombination occurs directly on (or in the vicinity of) the dopant sites initiated by a trapped hole, it is natural that it produces guest phosphorescence, which follows the charge recombination kinetics. In addition, charge carrier trapping by Btp$_2$Ir(acac) molecules can in an excellent way explain the more efficient quenching of the host fluorescence component in the electroluminescence spectra of CNPPP:Btp$_2$Ir(acac) OLEDs compared to the situation in photoluminescent spectra (Fig. 6.8(a) and (b)). Charge carrier trapping has often been used before to explain this phenomenon [328, 329]; however, in the present study direct evidence that the phosphorescent metal-organic complexes do act as charge traps was presented by means of TSL spectroscopy.

6.2 Optical Pumping of Triplet-Emitters

An important loss mechanism specific for electrically operating light-emitting devices under severe bias is singlet-triplet annihilation [50]. The longer lifetime of triplets compared to singlets and the fact that under electrical excitation much more triplets than singlets are generated, contribute to a high steady-state triplet density in the device. At high brightness conditions the triplet concentration can become high enough to quench singlets severely [50, 212, 215]. Using triplets for light-emission is an appealing solution to this problem.

In this section, the route of using triplet-emitters as light-emitting species in the active layer of an organic laser is investigated. The advantages are the smaller line-width of the spontaneous emission spectrum of phosphorescent compounds and the larger internal quantum efficiency [34]. As a result of both, the required current for lasing could be one order of magnitude smaller using triplet emitters. Lasing either by optical or electrical pumping of triplet-emitters, however, has not been demonstrated so far. Here, three different phosphorescent compounds are examined for signs of stimulated emission.

Fig. 6.12 Emission intensity and associated FWHM of a 600-nm thick PMMA:(2 wt%)$Btp_2Ir(acac)$ film measured at various pumping intensities. (Measurements performed by RWTH Aachen)

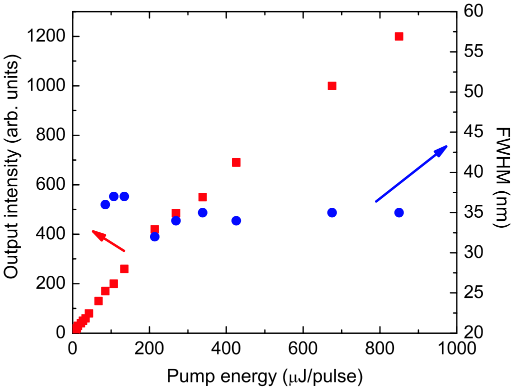

6.2.1 Attempts to Observe ASE Using $Btp_2Ir(acac)$

There are different options to check whether ASE can be observed from the commercially available phosphorescent metal-organic complex $Btp_2Ir(acac)$. The ideal situation is to use an inert film doped with a small concentration of the triplet-emitter. Because absorption is expected to be very low due to the low dopant level and the small extinction coefficient of $Btp_2Ir(acac)$, a relatively thick film should be used. Using a host-guest system, e.g. CNPPP:$Btp_2Ir(acac)$, could be another option. This has been carefully investigated in Sect. 6.1. Alternatively, ASE might be examined in diluted solution. All three possibilities were investigated.

First, $Btp_2Ir(acac)$ was dispersed in PMMA[3] and PS, which are considered as optically inert matrices. Both matrices were extensively studied for the dispersion of laser dyes, given their very good optical and thermal properties [125, 331]. A relatively thick film of 600 nm comprising 2 wt% $Btp_2Ir(acac)$ was prepared. Figure 6.12 shows the emission intensity of this film and the associated FWHM measured at various pumping intensities. Even at very high pumping intensities (well above 10 mJ/pulse) there could not be any increase of the slope efficiency observed. In fact, there was even a slight decrease of the emission intensity above 200 μJ/pulse, which might be attributed to sample degradation. In addition, no spectral narrowing was observed as indicated by a constant FWHM of the measured emission spectra. Similar results were obtained when a CNPPP:$Btp_2Ir(acac)$ film and a diluted solution of $Btp_2Ir(acac)$ molecules were optically pumped, indicating that it was impossible to obtain stimulated emission using the phosphorescent compound $Btp_2Ir(acac)$.

In order to identify the mechanism responsible for the lack of ASE, time-resolved pump-probe measurements were performed on a 4 μm thick PMMA:$Btp_2Ir(acac)$ film deposited on a quartz substrate. The sample was pumped at a wavelength of 400 nm, while the wavelength of the probe beam was set at the PL emission maximum $\lambda = 614$ nm. Figure 6.13 depicts the result of this experiment at an excitation

---

[3] Poly(methyl metacrylate).

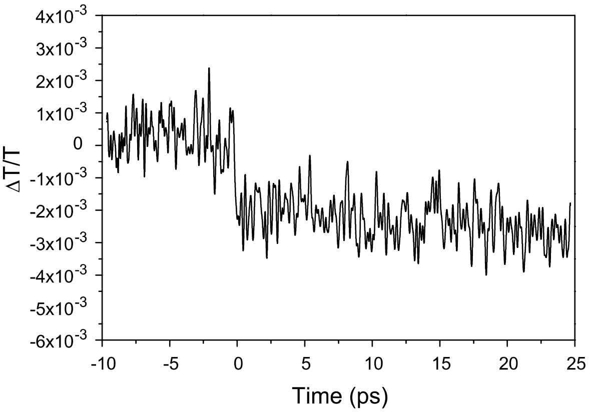

Fig. 6.13 Time-resolved pump-probe experiment carried out on a 4 μm-thick PMMA sample doped with 2 wt% $Btp_2Ir(acac)$. Sample excitation occurred at 400 nm using a laser fluence of 195 μJ/cm^2; the wavelength of the probe beam was set to 614 nm. (Measurements performed by RWTH Aachen)

laser fluence of 195 μJ/cm^2. As can be seen, a clear reduction in the transmission upon photo-excitation is measured. This observation indicates that $Btp_2Ir(acac)$ exhibits excited state absorption, which competes with radiative emission, and therefore prevents ASE. Due to fast intersystem crossing of singlets to triplet states, the excited state absorption of $Btp_2Ir(acac)$ is dominated by triplet-triplet absorption. These findings are in agreement with measurements reported by Adachi *et al.*, who demonstrated that several commonly-used Ir-complexes have large excited state absorptions [332] at the spectral region where light emission occurs. A cross-section for triplet-triplet absorption σ_{TT} of $3 \cdot 10^{-18}$ has been reported for $Btp_2Ir(acac)$, which is much larger than its $\sigma_{se} \simeq 7.9 \cdot 10^{-20}$ precluding any lasing action [332]. Apart from photoinduced absorption losses, also non-radiative losses such as quenching by oxygen and T-T annihilation due to the presence of movable host triplets (Sect. 6.1.1) may additionally deplete the triplet reservoir.

6.2.2 Attempts to Observe ASE Using F5Ph and GDP16b

The large σ_{TT} at the expected lasing wavelength of commercially available triplet-emitters, such as $Btp_2Ir(acac)$, might be problematic for achieving lasing action. In order to stand chance of obtaining ASE from triplet-emitters, the effective radiative lifetime has to be decreased (to have a larger cross-section for stimulated emission σ_{se}) or/and the spectral region where triplet-triplet absorption occurs has to be shifted with respect to the light emission spectrum. The metal-organic complexes F5Ph and GDP16b partially fulfill these requirements and were therefore optically pumped to check if ASE could be observed.

F5Ph was chosen because of its small radiative lifetime (~3 μs) compared to other triplet-emitters. However, its transient absorption spectrum overlaps with the spectral region where light-emission occurs. To check whether it is possible to observe ASE from F5Ph, two different experiments were performed. First, a thick (~1 μm) film of PMMA doped with 6 wt% F5Ph was measured. The results are

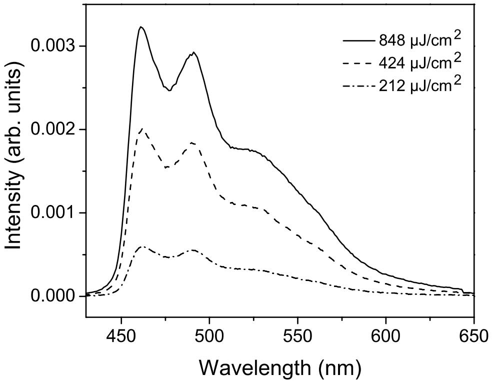

Fig. 6.14 Emission spectra of F5Ph for different laser fluences at 400 nm excitation wavelength. (Measurements performed by RWTH Aachen)

shown in Fig. 6.14. As can be seen, no spectral narrowing could be observed. Additionally, a diluted solution of 1 wt% F5Ph in de-aerated toluene has been measured at room temperature. Triplet-triplet annihilation and quenching of triplets by oxygen could definitely not be an issue in this case, however, no ASE was observed. We attribute these results to the high triplet-triplet absorption in the spectral region of interest.

In contrast to F5Ph, the metal-organic compound GDP16b exhibits triplet-triplet absorption which is reduced at the light-emission spectral range. The photoluminescence spectrum as well as the transient absorption spectrum of this compound are depicted in Fig. 6.15(a). Emission occurs in the range of 600–800 nm, which corresponds to a region of low transient absorption. Optical pumping of a thick PMMA film doped with 6 wt% GDP16b, however, failed to show spectral narrowing (Fig. 6.15(b)). This suggests that only reducing triplet-triplet absorption might not be enough to achieve lasing in triplet-emitters. Another possible explanation for the absence of ASE in GDP16b doped PMMA films, could be the presence of oxygen or the relatively high GDP16b dopant concentration.

6.3 Summary and Conclusions

In this chapter, triplet-emitter doped organic materials were studied. Triplet dynamics and charge carrier trapping in CNPPP and PS films incorporating the red-emitting metal-organic complex $Btp_2Ir(acac)$ were investigated. In addition, the intrinsic phosphorescence (Ph) of CNPPP was characterized. The results show that the decrease in the Ph efficiency in CNPPP:$Btp_2Ir(acac)$ systems at increasing excitation intensity is dominated by mutual host-guest triplet-triplet annihilation. Spectral diffusion effects were observed at 10 wt% of $Btp_2Ir(acac)$ dispersed in a polymer matrix, which is a direct proof of triplet migration though the manifold triplet-emitter sites at such dopant concentration level. This observation suggests straightforwardly that the concentration quenching observed in PS:$Btp_2Ir(acac)$ films arises due to triplet exciton migration at increased guest molecule concentration and thus

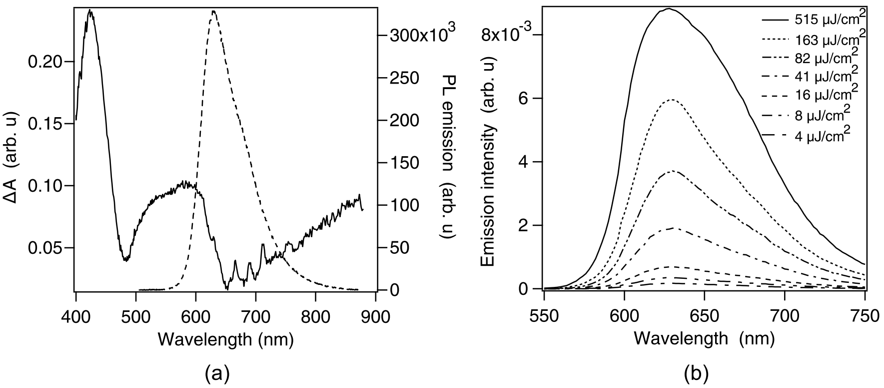

Fig. 6.15 (**a**) Emission spectrum (*dotted line*) and transient absorption spectrum measured at 400 ns delay time (*full line*) of GDP16b, and (**b**) emission spectra of a 6 wt% GDP16b doped PMMA film, measured at various laser fluences. (Measurements performed by RWTH Aachen)

their ability to encounter non-radiative oxygen impurities. A “delayed phosphorescence” was found in CNPPP:$Btp_2Ir(acac)$ films, which emerged at a time delay orders of magnitude larger than the natural lifetime of $Btp_2Ir(acac)$ triplet excitations. Delayed production of guest triplets by recombination of trapped charge carriers on $Btp_2Ir(acac)$ guest molecules was identified as the dominant mechanism for the observed delayed phosphorescence. The latter was supported by TSL measurements, which provided direct evidence that $Btp_2Ir(acac)$ creates hole traps in the conjugated polymer CNPPP. Good agreement between the experimentally obtained trap depth and the one predicted from the difference in HOMO levels was found.

In the second section of this chapter, the use of triplet-emitters as light-emitting species in the active layer of organic laser was investigated. Photoluminescence and time-resolved spectroscopic experiments on $Btp_2Ir(acac)$ showed the absence of amplified spontaneous emission, even when the samples were excited at very high pumping intensities. The reason for this behavior was attributed to an effective excited state absorption, which competes with radiative emission, and therefore prevents ASE. Additionally, two other metal-organic compounds, F5Ph and GDP16b, which exhibit, respectively, a relatively short radiative lifetime and a shifted transient absorption spectrum with respect to the emission spectrum were examined. However, also by using these compounds no spectral narrowing could be observed.